NIJEC 4 (2) (2025) 61- 78

NUML International Journal of Engineering and Computing

Journal Homepage: NIJEC.NUML.edu.pk
Print ISSN: 2788-9629

Design of Epi-RPNN for the Analysis of Bacteriophage Infection Model

Sabir Ali[a], Shahzad Khattak[b] *, Waseem[c], Faiza[d], Sabra Hafeez[e]

[a] Department of Mathematics, University of Waikato, Hamilton, New Zealand, 3240
[b] School of Mathematical Sciences, Jiangsu University, Zhenjiang, Jiangsu, China, 212013
[c] School of Mechanical Engineering, Jiangsu University, Zhenjiang, Jiangsu, China, 212013
[d] Department of Mathematics, Abdul Wali Khan University Mardan, Pakistan, 23200
[e] Department of Mathematics, COMSATS, Islamabad Campus, Pakistan, 44000

ARTICLE INFO

Article History:
Received 1 December 2025
Accepted 20 December 2025
Available Online 6 January 2026

Keywords:
Bacteriophage infection, Nonlinear Dynamics, Random projection neural network, Nonlinear optimization, Efficacy, Absolute error.

Funding:
This research received no specific grant from any agency in public, commercial or non-for-profit sector

Conflict of Interest:
The author has declared no potential conflicts of interest and falsification/fabrication of data with respect to the research, authorship, and/or publication of this article.

ABSTRACT

In this study, we examine the analysis with accuracy based on intelligent computing for the bacteriophage infection model frequently employed in epidemiology. The microbiological is an interesting phenomenon known as bacteriophage infection or phage infection. Bacteriophages are viruses that target and infect bacteria specifically, then use the bacteria as hosts for their own replication. By injecting their genetic material into the bacterial cell, these phages cause the host cell's machinery to be redirected in order to produce more phages, which ultimately causes the lysis or obliteration of the bacterial host. The derivation of the basic reproduction number and numerical simulations are conducted through a new machine learning approach called the random projection neural network (RPNN) method. The accuracy and robustness of our methodology are examined through a comparison of the results with numerical solvers ode23t and ode15s available in MATLAB. Moreover, the data testing, training and validation of mean square error are examined through performance, training test, error histogram, regression and fitness plots.

1. Introduction

The term "bacteriophage" or "phage" refers to a virus that may spread and infect bacteria. Frederick Twort and Felix d'Herelle discovered bacteriophages in 1915 [1] and 1917 [2], respectively.

Bacteriophages are made up of a protein-coated capsid and a genetic material (nucleic acid) core. The two life cycles that phages typically follow are lytic (virulent) and lysogenic (temperate). Lytic phages attack bacteria by attaching their tails to their surface and then injecting DNA into the bacterium from their heads. As new daughter phages are produced as a result of the host bacteria's raw materials being used to biosynthesize the DNA that enters the bacteria. These phages cause bacterial cells to explode after they reach a specific number, at which point they can replicate quickly and produce hundreds of daughter phage particles.

https://doi.org/10.52015/nijec.v4i2.114

Lysogenic phages integrate their nucleic acid into the host cell's chromosome and multiply alongside it in tandem without harming the host cell. Lysogenic phages, for which a lytic cycle occurs, can be induced under specific circumstances. The process of infecting more bacterial cells by each daughter phage is done repeatedly, allowing the phages to kill a large number of cells. Phage therapy has been used to treat infections caused by harmful bacteria for a long time. Phage therapy has been utilized extensively in many industries, including the breeding of livestock and poultry [3, 4], aquaculture [5] food production [6], and other fields [7, 8]. Also, antibiotic resistance is a global health threat, and phage therapy is a safe and effective treatment method.

However, there is no bibliometric analysis of trends on this topic [9]. The reference [10] presents a mathematical model that consider bacteria, phages, and the innate immune response with a discrete time delay. It determines local and global stability of equilibria, Hopf bifurcation, and bifurcating periodic solutions. A model uses the normal form method and center manifold theory for precise expressions. Phage therapy, an alternative to antibiotic chemotherapy, is being evaluated for its efficacy in preclinical animal models to combat bacterial resistance [11]. A patient with a Pseudomonas aeruginosa multidrug-resistant prosthetic vascular graft infection was treated with phages and ceftazidime-avibactam. However, a new BSI occurred without antimicrobial therapy, involving a wild-type strain susceptible to β-lactams and quinolones. Analysis revealed a clonal relationship with phage administration, genomic changes, and decreased MICs to B-lactams and quinolones [12].

A new P. aeruginosa bloodstream infection occurred without antimicrobial therapy after phage treatment, with a wild-type strain susceptible to B-lactams and quinolones, revealing genomic changes and increased biofilm production [13, 14]. Moreover, phage therapy has proved to be an effective treatment for human diseases such as wound infections caused by skin facultative pathogens such as staphylococcus and streptococcus, and diarrheal diseases caused by e. coli, shigella, or vibrio. Phage therapy has recently been applied to the treatment of systemic and even intracellular illnesses. Since the discovery of phage 100 years ago, phage research has continued unabated. Phage therapy gradually lost popularity as antibiotics became more widely used. However, the widespread development of bacterial drug resistance in recent years has heightened interest in bacteriophage research.

It's still debatable whether phages can completely replace antibiotics as a new way to treat bacterial illnesses, and it will probably take some time before they start showing up in clinical studies. Finding a theoretical foundation for research into the interaction between phage and bacteria is a challenge of enormous significance and difficult complexity. The goal of this work is to examine the link between phages and bacteria, simulate the dynamic stability of phage-infected bacteria, and offer some theoretical support for the claim that phages may effectively treat, prevent, and control infectious diseases. Also to get the best results through numerical simulation physics-informed neural networks methodology has been adopted. Pages can be considered parasitic organisms that host bacteria or predatory species that feed on them.

There are numerous dynamical models of viral infection in host cells, to the best of our knowledge [15,16]. For instance, Ebert et al. Also, phage therapy model without and with time delay [17]. [18] ignored the potential of host recovery when they considered a model of microparasite transmission for a horizontally transmitted parasitic and constructed the host-born density-dependent cabin model. The model is stated as:

$$\begin{aligned} \phi(t) &= r(\phi + f\psi)[1 - c(\phi + \psi)] - \mu\phi - \beta\psi\phi \\ \psi'(t) &= \beta\psi\phi - (\mu - \nu)\psi, \end{aligned} \tag{1}$$

where, at time t, ϕ, and ψ represent, respectively, the densities of susceptible and infected (infective) hosts; The maximum per capita birth rate of uninfected hosts are represented by the parameter r. Other variables include the relative fecundity of infected hosts, μ, β, and ν, which

measure the excess death rate brought on by the parasite as a function of host density. According to this model, there will always be an equilibrium between infected and uninfected hosts, and the population will move towards this equilibrium either monotonically or through damped oscillations.

This research is about the new modified form of Elbert's model by presuming that infected hosts (bacteria) can reproduce according to the logistic law, and investigate a class of parasites (phages) infection models. The model is stated following:

$$S'(t) = r_1\left(\frac{M-S-I}{M}\right)S - d_1 S - \beta S I \qquad S(0) = C1$$
$$I'(t) = \beta S I + r_2\left(\frac{M-S-I}{M}\right)I - (d_1 + e)I \qquad I(0) = C2, \tag{2}$$

Here, d_1 stands for the phage-independent bacteria background mortality is the proportionality coefficient of parasite infection, and denotes the phage-induced excess death rate. r_1, r_2 are the proliferation constants of uninfected and infected hosts, respectively, and Mis the environmental tolerance of a host population. The total number of population N for this model is the composition of two classes of infected and uninfected hosts i.e. $N(t) = I(t) + S(t)$ respectively. The logistic growth of the uninfected and infected microbes is given by $r_1S(t)\,[1 - (S(t) + I(t)) / M$ and $r_2I(t)\,[1 - (S(t) + I(t))/ M$, respectively. Discussion about positively invariant sets and equilibria and stability analysis (global and local stability) are given in referenced in [19]. According to [19], stability is analyzed by Bendixson–Dulac theory and Jacobian matrix.

1.1 Novelty and Contribution

In previous studies, theoretical analyses have been presented for Elbert's modified model so far, but this analysis is based on the computational intelligence paradigm. In the present time, the application of the random projection neural network is rare in epidemiology. In this paper, our primary goal is to analyze the modified Elbert's model for bacteriophage infection by using the random projection neural network (RPNN). This framework is present to optimize the prevention, control, and treatment of infectious diseases caused by phages. The efficacy of our proposed method is examined by comparing it with the MATLAB solvers. This article is organized as follows:

a. Section 2 is about the basic reproduction number $R_0(\beta)$
b. The RPNN methodology is given in section 3
c. Numerical simulations are given in section 4
d. Results and Discussion are given in section 5
e. The section 6, contains the concluding remarks.

2. Basic Reproduction Number

In this section, the primary reproduction number, say $R_0(\beta)$ is derived from model (2), using the next-generation matrix method [20].

$$F = \beta\overline{S} + r_2\left(\frac{M-\overline{S}}{M}\right) \qquad V = d_2, \tag{3}$$

The method of the next-generation matrix is

$$FV^{-1} = \frac{1}{d_2}\left[\beta\overline{S} + r_2\left(\frac{M-\overline{S}}{M}\right)\right] \tag{4}$$

Consequently, the fundamental reproduction number is given by

$$R_0(\beta) = \frac{1}{d_2}\left[\beta\overline{S} + r_2\left(\frac{M-\overline{S}}{M}\right)\right] \tag{5}$$

$R_0(\beta)$ is obviously increasing in beta, and $R_0(c)$ equals 1, where $\beta_c = \omega/r_1\bar{S}$.

$$d_2(R_0(\beta) - 1) = \beta\bar{S} + r_2\left(\frac{M-\bar{S}}{M}\right) - d2 \tag{6}$$

Theorem 2.1:Under the assumptions and notations of Propositions 2.1–2.2 in [19], the following statements are true:

a. If $R_0(\beta) < 1$, thenE1 is locally asymptotically stable;

b. If $R_0(\beta) > 1$, thenE1 is a saddle and unstable.

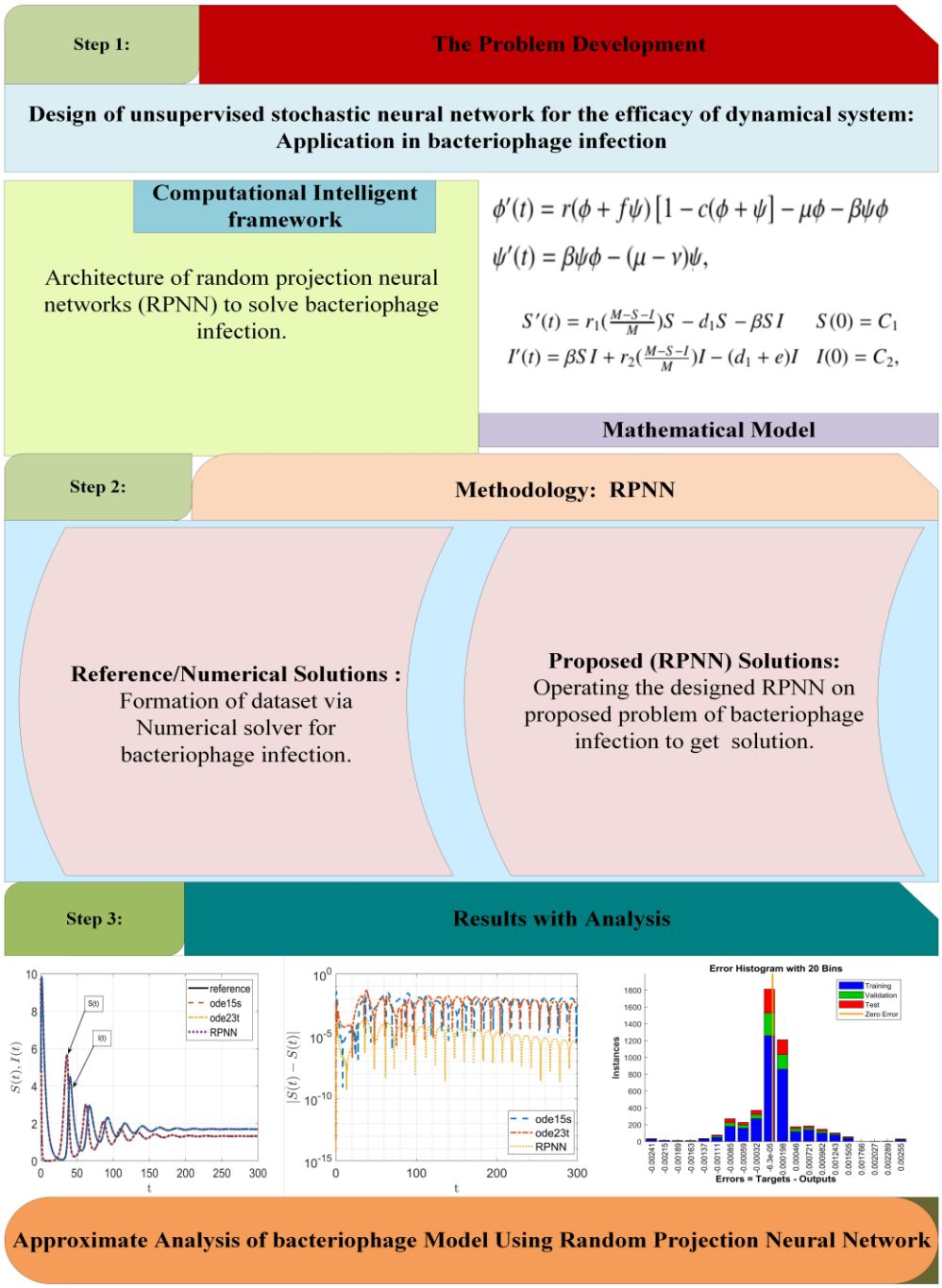

Figure1: Graphical abstract for RPNN approach to study bacteriophage infection.

3. Designed Random Projection Neural Network (RPNN) Methodology

The analysis of biological models with the help of random projection neural network (RPNN) with initial conditions taking into account [21]. The RPNN approach for a set of first-order differential equations is presented here in mathematical form. The structure of RPNN methodology is presented in Figure.2.

Consider a system of differential equations of the first order as follows:

$$\frac{du}{dt} = f(u,t), \tag{7}$$

where t is the independent variable (time), u is a vector of dependent variables, and f is a vector-valued function. The solution $u(t)$ is approximated by a neural network using the RPNN methodology. The neural network looks like this:

$$u(x) \approx u_{N\,N}(x,t) = W_2 \,.\, \sigma(W_1 \,.\, x + b) + b_2 \tag{8}$$

Where W_1 and W_2 are weight matrices, b_1 and b_2 are bias vectors, and σ is an activation function; x represents the input features; and u_{NN} (x, t) is the neural network approximation of the solution. A random projection technique is used to minimize the differential equation's residual in order to impose the physics-based requirements. In order to do this, random samples of the input feature x must be taken, and the following optimization problem must be resolved:

$$min W_1, W_2, b_1, b_2 \sum_{i=1}^{N} \| \frac{du_{NN}(x_i,t)}{dt} - f(u_{NN}(x_i,t),t)\|^2 \tag{9}$$

Where N is the total number of samples, and x_i is the i^{th} sample of the input features.

Usually, gradient-based optimization methods like stochastic gradient descent (SGD) or Adam-Jacobin are used to address the optimization problem. Backpropagation is used to calculate the gradients of the objective function concerning the weights W_1, W_2, and b_1, b_2, and the parameters are updated iteratively until convergence. The RPNN methodology offers an approximation $u_{NN}(x, t)$ that satisfies the proposed model. The RPNN approach efficacy may change based on the situation and the particular problem being addressed. A general mathematical framework for comprehending the methodology is provided by the aforementioned statement.

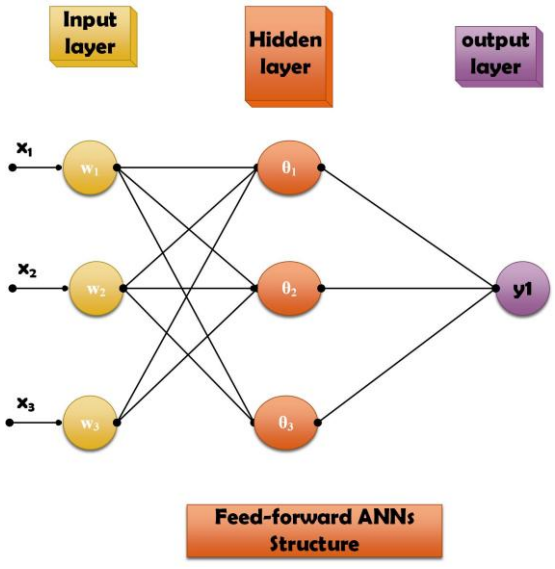

Figure 2: General Structure of Random Projection Neural Networks

4. Numerical Simulation

In numerical simulation, five individual case studies are presented based on making variations in parasite infection's coefficient β in system 2 with input domain t ∈ [0, 300]. For each case study, two MATLAB solvers, ode15s and ode23t, have been considered for comparison to assess the accuracy of the proposed method. The simulation is processed through the RPNN methodology.

The first step towards the simulation is formulating the approximate solution using a specific activation function for system2regarding the current methodology. The equation (8) can be written as follows:

$$\hat{S}(t) = \sum_{j=1}^{m} \varphi_j \left(e^{-(\omega_j t+\beta j)^2}\right),\ \hat{I}(t) = \sum_{j=1}^{m} \varphi_j \left(e^{-(\omega_j t+\beta j)^2}\right), \tag{10}$$

$$\hat{\dot{S}}(t) = \sum_{j=1}^{m} -\varphi_j\left(2\omega^2 j + 2w_j b_j\right)\left(e^{-(\omega_j . t+\beta j)^2}\right), \hat{\dot{I}}(t) = \sum_{j=1}^{m} -\varphi_j\left(2\omega^2 j + 2w_j b_j\right)\left(e^{-(\omega_j . t+\beta j)^2}\right). \tag{11}$$

The equation (10) and (11) are the approximate solutions for S(t) and I(t), and its derivatives respectively. Where β = [β_1, β_2, β_3, . . . , β_m], $\varphi = [\varphi_1, \varphi_2, \varphi_3 . . ., \varphi_m]$, and w= [$\omega_1$, ω_2, ω_3, . . ., ω_m] are unknown weights that is to be determine.

The equation (9) represents the mean square error (MSE) and is written for the system 2 as follows:

$$\begin{aligned} \epsilon = & \frac{1}{N}\sum_{m=1}^{N}\left(\hat{S'}_m - 0.4\left(\frac{10-\hat{s}_m-\hat{I}_m}{10}\right)\hat{S}_m + 0.01\hat{S}_m + B\hat{S}_m\hat{I}_m\right)^2 \\ & + \frac{1}{N}\sum_{m=1}^{N}\left(\hat{I'}_m - B\hat{S}_m\hat{I}_m - 0.4\left(\frac{10-\hat{s}_m-\hat{I}_m}{10}\right) + (0.01+0.2)\,\hat{I}_m\right)^2 \\ & + \frac{1}{2}\left((\hat{S}_0 - 9.75)^2 + (\hat{I}_0 - 4.75)^2\right), \end{aligned} \tag{12}$$

Where N=1/h, $\hat{S}_m = \hat{S}(t_m)$ and $\hat{I}_m = \hat{I}(t_m)$. The values for all parameters in equation (12) are tabulated in Table1 (see [18]). As stated, before that the accuracy of the approximate solution is defended on absolute errors "ϵ". When ϵ approaches zero implies that the approximate solution approaches the exact solution.

The five different case studies are listed below:

a. Case study 1: β=0.0180, r_1 =r_2 =0.4, M=10, e=0.2 and d_1 =0.01
b. Case study 2: β=0.0520, r_1 = r_2 =0.4, M=10, e=0.2 and d_1 =0.01
c. Case study 3: β=0.0390, r_1 = r_2 =0.4, M=10, e=0.2 and d_1 =0.01
d. Case study 4: β=0.0238, r_1 =0.4, r_2 =0, M=10, e=0.2 and d_1 =0.01
e. Case study 5: β=0.1580, r_1 =0.4, r_2 =0, M=10, e=0.2 and d_1 =0.01

Each case study undergoes the same procedure after the simulation process.

5. RESULTS AND DISCUSSION

We proposed a novel RPNN methodology for this research study with two MATLAB ODE solvers, ode15s and ode23t. The main purpose behind selecting these solvers is to assess the accuracy and robustness of our proposed method. The comparison between the required results is conducted

through figures and tables. Required results are obtained using equations (10,11) for domain [0,300] with step-size h=0.0001. Find out the best-optimized weights for each case study and substitute these weights in equations (10-11), and substitute these values in equation (12) to minimize the MSE. The discussions on the required results are presented as follows:

Table 1: Parameters that are involved in system 2

Parameters	Physical interpretation	Values
d_1	background mortality of hosts	0.01
e	Increased death rates parasite-induced	0.2
M	Environmental tolerance of a host population.	10
r_1	proliferation constant of un-infected hosts	0.4
r_2	proliferation constant of infected hosts	0.4, 0
C_1	Initial condition for $S(t)$	9.75
C_2	Initial condition for $I(t)$	4.75

5.1 Case Study 1

The solution is obtained with carrying suitable weights by using the novel RPNN technique. The proposed solutions for un-infected hosts *S(t)* is presented in Figure. 3a that is approaches to the initial conditions for $\hat{S}(t)$ in the system (2). The absolute errors (AEs) for un-infected hosts are presented in Figure. 3b. The Infected hosts $\hat{I}(t)$ is shown in Figure. 4a and the respective AEs are given in Figure. 4b, we observed that the lowest value for AEs is obtained on $t \approx 0.01$ value. The solutions are approaches to positively stable points (0, 9.75). The numerical results of absolute errors (AEs) are stated in Table 2. The lowest errors have been achieved as compared to the other two MATLAB solvers and also for the reference line. The accuracy of this case study is $E-14-E-06$ for both infected and uninfected hosts.

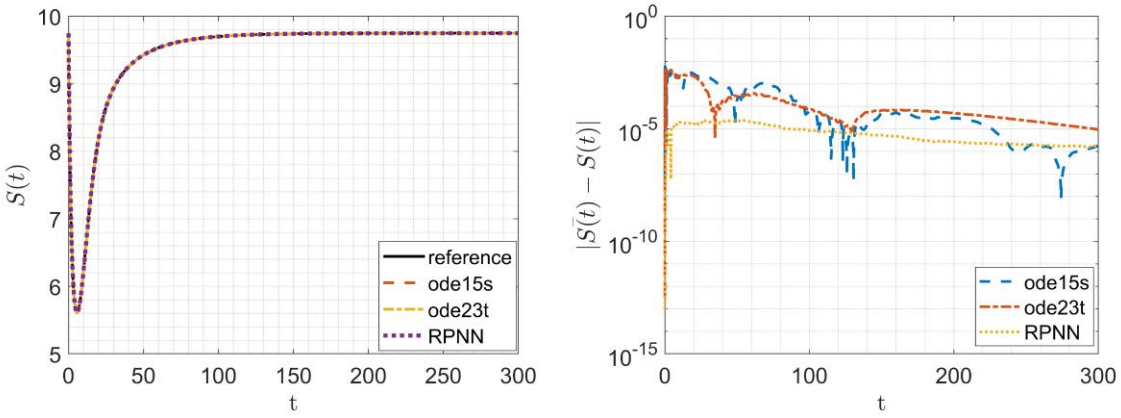

(a) Solution $S(t)$ (b) Absolute Errors $S(t)$

Figure 3. Approximate Solutions and Absolute Errors for Un-Infected Hosts $S(T)$, Case Study 1

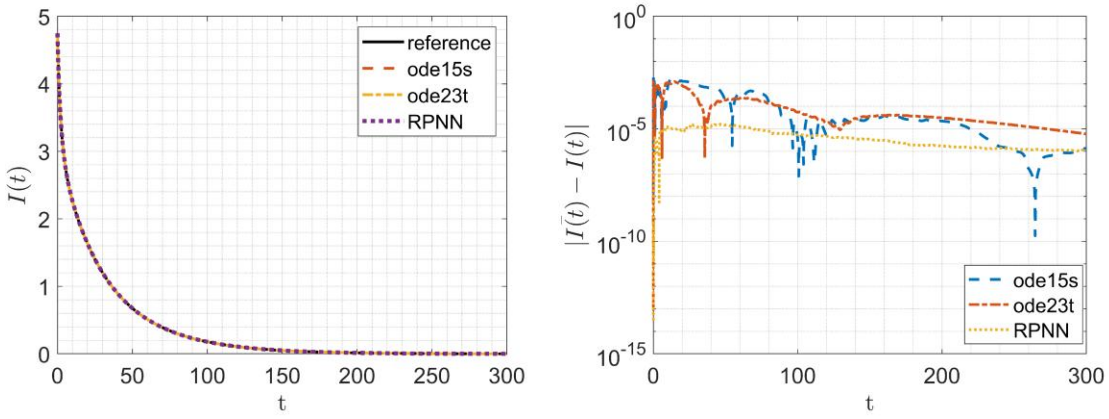

(a) Solution $I(t)$ (b) Absolute Errors $I(t)$

Figure 4. Approximate Solutions and Absolute Errors for Un-Infected Hosts $I(T)$, Case Study 1

Table 2: Comparison of Minimum Absolute Errors for $\beta = 0.018$, Case Study 1

t	$AE\ \ St)$			$AE\ \ I(t)$		
	ode15s	ode23t	RPNN	0de15s	ode23t	RPNN
0.00	0	0	0	0	0	0
30	4.57E-08	2.81E-13	9.24E-14	2.70E-08	3.90E-13	4.00E-14
60	1.54E-06	4.24E-10	4.17E-13	6.31E-07	2.42E-10	1.63E-13
90	0.000496	4.53E-05	1.16E-11	2.75E-06	4.61E-09	1.17E-12
120	0.006898	0.003884	1.48E-10	2.33E-05	3.34E-07	1.09E-11
150	0.009163	0.003509	1.58E-09	0.00022	3.06E-05	1.08E-10
180	0.009163	0.003509	1.58E-09	0.001161	0.001206	1.04E-09
210	0.008152	0.002044	1.08E-07	0.002538	0.001158	1.07E-08
240	0.003304	0.000106	1.28E-06	0.002079	0.000827	1.03E-07
270	0.001934	0.001042	3.39E-06	0.000512	0.000131	1.27E-06
300	1.74E-06	9.23E-06	2.26E-06	1.36E-06	5.85E-06	1.54E-06

5.2 Case Study 2

The approximate solution is obtained by considering the parameter β = 0.052 that is shown in Figure. 5a. After minimizing the equation (12), the obtained minimum AEs for uninfected hosts are shown in Figure. 5b. Also, the graphical representation of approximate solutions of infected hosts and the respective AEs are presented in Figure. 6a, and 6b respectively. The initial conditions are verified by the results for both infected and uninfected cases and approaches to stable points (0, 4.75). The numerical values of this case study are tabulated in Table 3. Moreover, the accuracy of our outcomes is E – 14 – E – 06 and E– 15 – E – 06 for uninfected S (t) and infected I(t) respectively.

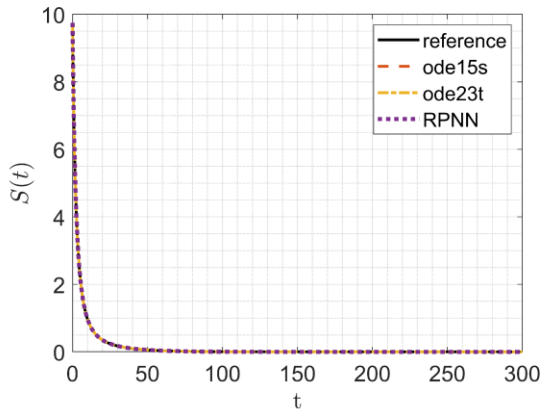

(a) Solution $S(t)$

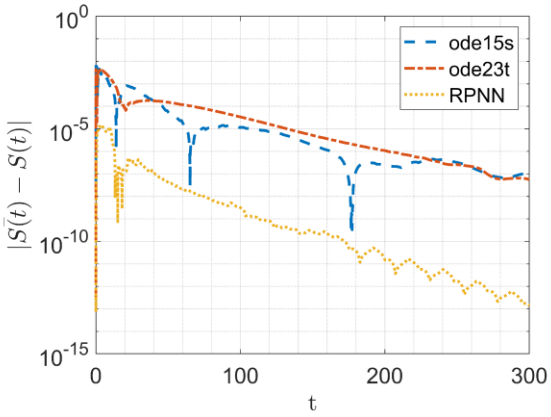

(b) Absolute errors $S(t)$

Figure 5: Approximate solutions and absolute errors for un-infected hosts $S(t)$, case study 2

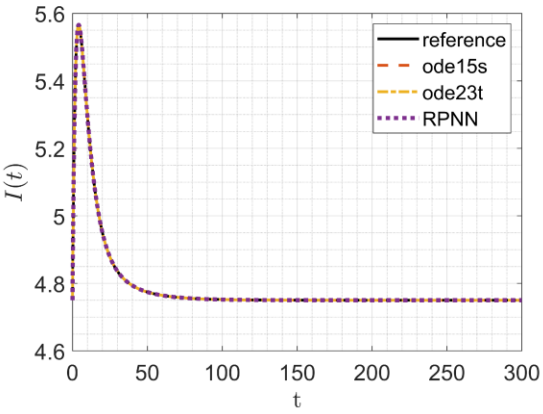

(a) Solution I(t)

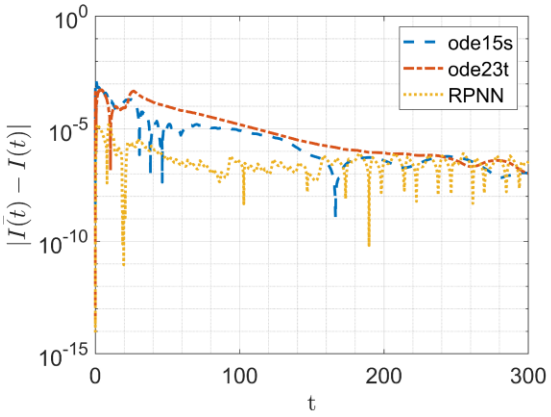

(b) Absolute Errors I(t)

Figure 6: Approximate Solutions and Absolute Errors for Un-Infected Hosts $S(T)$, Case Study 2

Table 3: Comparison of minimum Absolute Errors for $\beta = 0.052$, case study 2

t	$AE\ \ St)$			$AE\ \ I(t)$		
	ode15s	ode23t	RPNN	0de15s	ode23t	RPNN
0.00	0	0	0	0	0	0
30	4.72E-08	2.93E-13	9.59E-14	4.53E-09	2.84E-14	9.77E-15
60	9.45E-08	1.37E-12	1.87E-13	9.05E-09	1.31E-13	1.95E-14
90	4.72E-05	3.90E-07	1.19E-12	1.01E-05	1.87E-07	1.48E-12
120	0.001036	0.000198	2.57E-11	7.97E-05	1.21E-05	1.34E-11
150	0.002912	0.001786	1.11E-10	0.000323	0.000239	1.07E-10
180	0.007809	0.003921	2.49E-09	0.001148	0.000299	5.06E-09
210	0.010228	0.003744	1.10E-08	0.001245	0.00025	1.04E-08
240	0.009702	0.003177	1.06E-07	0.001498	0.000126	1.07E-07

t	$AE\ \ S(t)$			$AE\ \ I(t)$		
	ode15s	ode23t	RPNN	0de15s	ode23t	RPNN
270	0.003034	0.000227	1.78E-06	0.001102	0.000144	1.59E-06
300	9.61E-08	5.59E-08	4.45E-12	1.04E-07	1.07E-07	5.23E-07

5.3 Case Study 3

By varying the value of parameter β and the considering the suitable weights in equations (10,11), the compatible solution is obtained. The required approximate solutions and optimized mean square errors for uninfected hosts are shown in Figure 7a and Figure 7b respectively. As observed that the required solutions satisfied the respective initial conditions. The infected hosts I(t) solution is shown in Figure. 12, that clearly indicate the initial conditions are satisfied. The respective AEs are represented in Figure. 8a. Both solutions of uninfected and infected hosts are approaches to positively stable values (0.38, 4.75) follows by Figures. 7a & 8a. According to these statistics, the lowest MSEs have been obtained as compared to the other state of the art. The values of our required approximate solutions are stated in Table 4. The accuracy of proposed technique for this case study is E − 14 − E − 06 and 0 − E − 16 − E − 07 regarding uninfected and infected hosts.

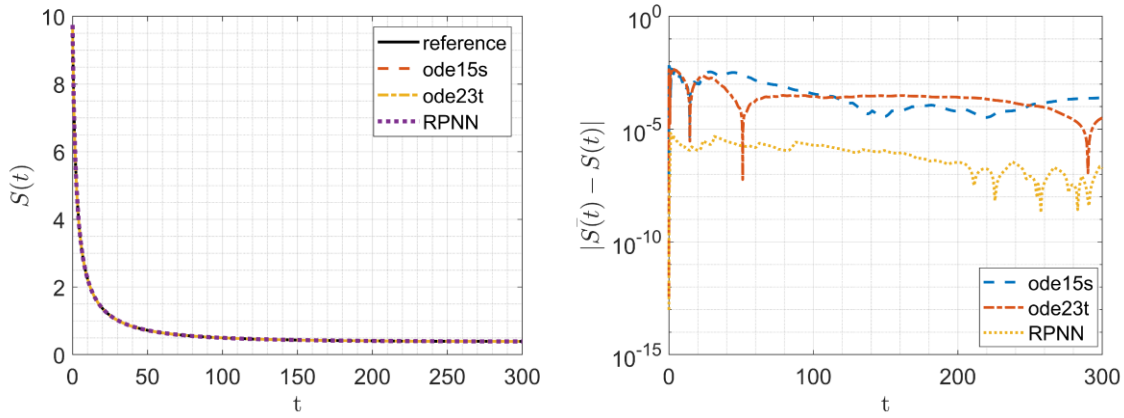

(a) Solution $S(t)$ (b) Absolute errors $S(t)$

Figure 7: Approximate Solutions and Absolute Errors for Un-Infected Hosts $S(t)$, Case Study 3

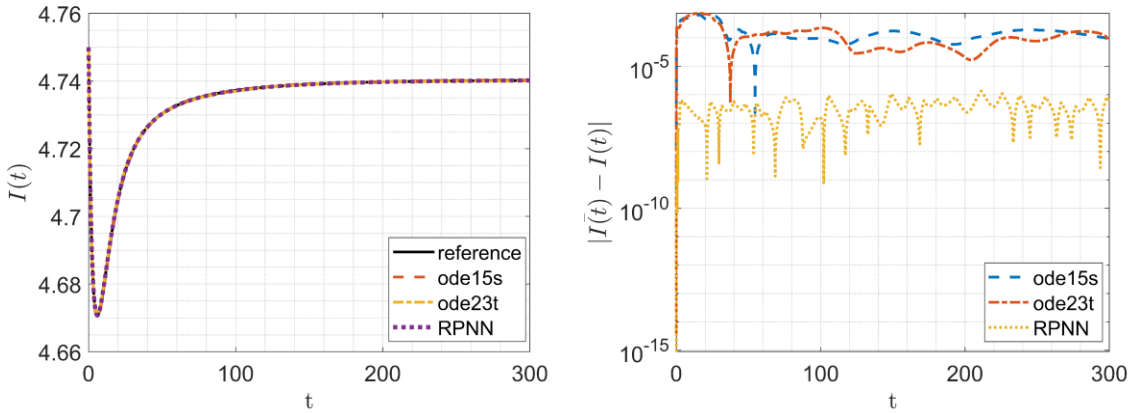

(a) Solution $I(t)$ (b) Absolute Errors $I(t)$

Figure 8: Approximate Solutions and Absolute Errors for Un-Infected Hosts $S(T)$, Case Study 3

Table 4: Comparison of minimum Absolute Errors for $\beta = 0.039$, case study 3

t	$AE\ \ S(t)$			$AE\ \ I(t)$		
	ode15s	ode23t	RPNN	0de15s	ode23t	RPNN
0.00	0	0	0	0	0	0
30	4.70E-08	2.91E-13	9.77E-14	4.48E-10	3.55E-15	8.88E-16
60	9.40E-08	1.36E-12	1.85E-13	1.34E-09	3.20E-14	1.78E-15
90	6.48E-05	7.36E-07	1.15E-12	2.06E-07	7.83E-10	0
120	0.000709	9.12E-05	1.12E-11	2.64E-07	1.28E-09	8.88E-16
150	0.003361	0.002518	1.10E-10	1.87E-05	7.19E-06	3.06E-12
180	0.007173	0.004067	1.10E-09	3.58E-05	3.16E-05	1.99E-11
210	0.009669	0.003224	1.03E-08	2.57E-05	7.47E-05	2.65E-10
240	0.005405	0.000653	1.01E-07	0.000264	0.000231	6.37E-09
270	0.001438	0.00115	1.40E-06	0.000325	0.000203	4.48E-08
300	0.000246	3.16E-05	1.78E-07	9.48E-05	8.10E-05	5.18E-07

5.4 Case Study 4

For this case study, the value of parameter $\beta = 0.0238$ is taken in to count. The RPNN method is tested to obtain the approximate solution. The required approximate solutions for $S(t)$ and $I(t)$ in one Figure. 9a and 10a. Both graphs verified the respective initial conditions. Both required solutions are approaches monotonically to stable points (8.9, 0.7) for $S(t)$, $I(t)$ respectively. The minimized AEs for $S(t)$ are presented graphically in Figure. 9b and the AEs for $I(t)$ are shown in Figure. 10b. All AEs of case study 4 are combined listed in Table 5. The lowest error is $E-14-E-06$, which is compatible as compared to other referenced methods.

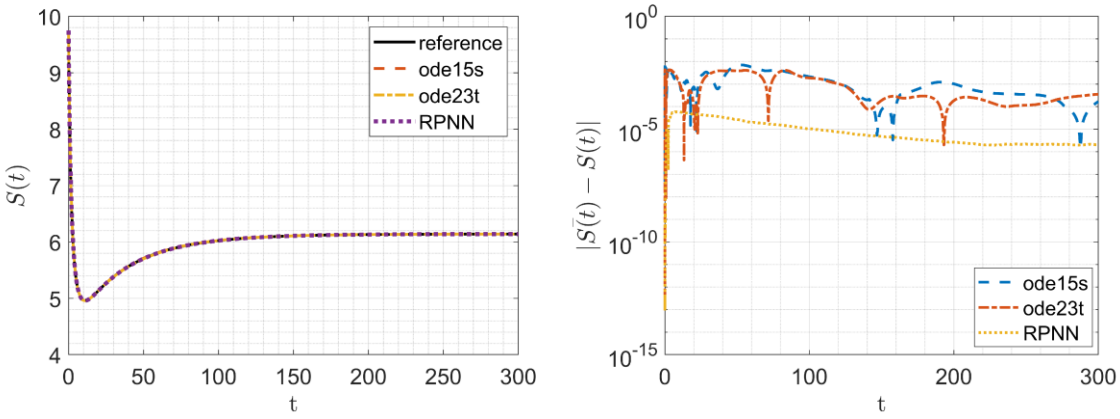

(a) Solution $S(t)$ (b) Absolute errors $S(t)$

Figure 9: Approximate solutions and absolute errors for un-infected hosts $S(t)$, case study 4

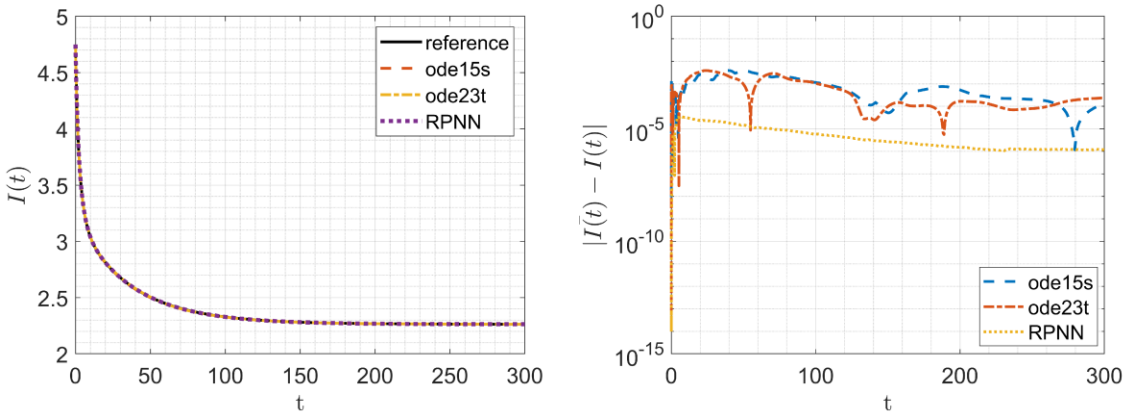

(a) Solution $I(t)$ (b) Absolute Errors $I(t)$

Figure 10: Approximate Solutions and Absolute Errors for Un-Infected Hosts $S(t)$, Case Study 4

Table 5: Comparison of Minimum Absolute Errors for β = 0.0238, Case Study 4

t	$AE\ \ S(t)$			$AE\ \ I(t)$		
	ode15s	ode23t	RPNN	0de15s	ode23t	RPNN
0.00	0	0	0	0	0	0
30	4.67E-08	2.88E-13	9.06E-14	1.83E-08	2.66E-13	3.38E-14
60	9.35E-08	1.35E-12	1.74E-13	1.85E-06	3.06E-09	1.40E-13
90	1.55E-05	4.20E-08	1.18E-12	8.88E-06	7.10E-08	1.02E-12
120	0.000116	2.38E-06	1.15E-11	8.25E-05	6.24E-06	1.05E-11
150	0.001519	0.000441	1.62E-10	0.000533	0.000303	1.01E-10
180	0.005418	0.004211	1.03E-09	0.001283	0.000808	1.00E-09
210	0.008756	0.002768	1.87E-08	0.001607	0.000835	1.04E-08
240	0.00706	0.001874	1.37E-07	0.001195	0.000619	1.01E-07
270	0.002561	0.000282	1.19E-06	0.000337	9.19E-05	1.34E-06
300	0.000168	0.000355	2.06E-06	0.000136	0.000235	1.20E-06

5.5 Case Study 5

The approximate solutions for both uninfected and infected hosts are shown in Figure. 11a and 12a for β = 0.158. As noted, both approximate solutions are approaches to equilibrium point (1.4,1.87) by damped oscillations. The required solutions are completely verified with initial conditions. The absolute errors of Sˆ(t) and MSEs of Iˆ(t) are shown in Figure. 11b and Figure. 12b respectively. The Table 6 represent the error. According to Table 6, RPNN method obtained the lowest residue errors. The accuracy of our proposed technique for uninfected hosts S (t) is E − 15 − E − 06 and the accuracy for infected hosts I(t) is E − 14 − E − 06.

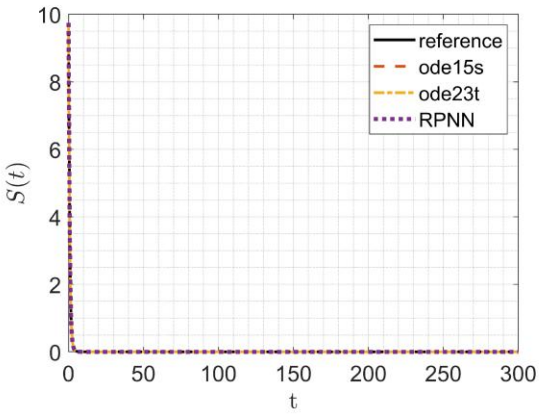

(a) Solution $S(t)$

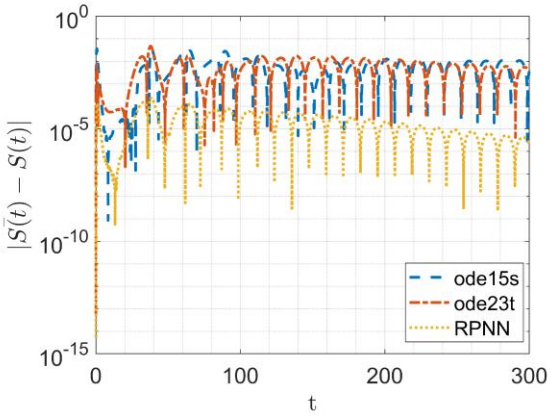

(b) Absolute errors $S(t)$

Figure 11: Approximate Solutions and Absolute Errors for Un-Infected Hosts $S(t)$, Case Study 5

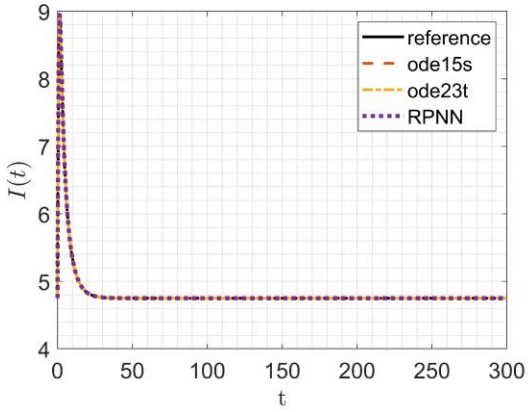

(a) Solution $I(t)$

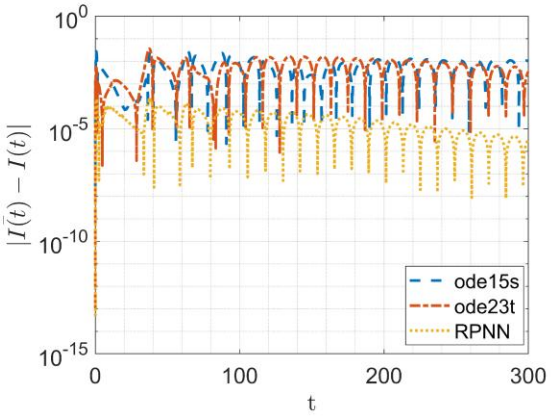

(b) Absolute Errors $I(t)$

Figure 12: Approximate Solutions and Absolute Errors for Un-Infected Hosts S(t), Case Study 5

Table 6: Comparison of Minimum Absolute Errors for $\beta = 0.0238$, Case Study 5

t	$AE\ \ S(t)$			$AE\ \ I(t)$		
	ode15s	ode23t	RPNN	0de15s	ode23t	RPNN
0.00	0	0	0	0	0	0
30	6.08E-09	5.51E-14	1.78E-15	3.27E-08	4.27E-13	9.50E-14
60	1.22E-08	2.18E-13	3.55E-15	4.91E-08	1.03E-12	1.39E-13
90	4.48E-08	2.99E-12	3.73E-14	7.06E-06	2.41E-08	1.15E-12
120	2.82E-07	1.19E-10	2.22E-13	6.88E-05	2.33E-06	1.09E-11
150	1.53E-06	3.51E-09	1.28E-12	0.000661	0.000268	1.15E-10
180	1.56E-05	3.58E-07	1.25E-11	0.001122	0.001085	7.03E-10
210	0.00013	2.33E-05	1.06E-10	0.006025	0.002593	1.80E-05
240	0.000748	0.000574	2.10E-09	0.010967	0.004074	4.84E-05

t	$AE\ \ S(t)$			$AE\ \ I(t)$		
	ode15s	ode23t	RPNN	0de15s	ode23t	RPNN
270	0.002636	0.001326	1.95E-07	0.018686	0.005553	0.000117
300	0.003606	0.003739	1.97E-06	0.010041	0.00349	3.23E-06

Computational complexity analysis of a modified model of bacteriophage infection through RPNN methodology. We analyzed different aspects of phage infection. Five individual case studies are adopted for numerical simulation. This numerical simulation is conducted through MATLAB R2021a. A total of 2826 runs are adopted for this MATLAB simulation to calculate the complexity of this model. The total execution time for each case study is 1.793492 seconds, as shown in Table 7. The methods, Retol, L2rr, Execution time in seconds, and steps are tabulated in Table 7. This simulation is performed on a Dell latitude laptop with 8 GB RAM, 500 SSD, having a 64-bit operating system core i5 and x64-based processor.

Table 7: Performance of the Methods in Comparison to RPNN for Each Case Study.

Methods	Retol	L2err	Exec_time in sec	Steps
'ode15s'	0.001	0.228499	0.23593	87
'ode23t'	0.001	0.125409	0.201442	107
'RPNN'	0.001	0.00541	1.793492	68
'reference'	1.00E-14	0	2.59492	3030

6. CONCLUSION

The main theme of our study is to analyze the infectious bacteria-phage dynamical model through the novel RPNN scheme. The parasite (phage) population is not explicitly modeled, which is a striking feature of this model. We evaluated the model with a new machine learning approach known as a random projection neural network RPNN. Five different cases were established based on our study of host-parasitic relationships: both infected and uninfected hosts become extinct simultaneously, resulting in the extinction of infected hosts, and Uninfected and infected hosts co- exist, resulting in the extinction of uninfected hosts. In particular, we have examined the instability of the extinction equilibrium for the given model. Moreover, E_1 is locally asymptotically stable if $R_0 < 1$.

We have compared the obtained results with state of the art, which proves the efficacy of our designed methodology for the given model. The simulation shows that our methodology is suitable than the other MATLAB solvers. Also, the LMANNs are implemented through MATLAB tool for testing, training and validation process. In the future, we will apply RPNN to other biological disease models and different chaotic systems. Certainly! Let's break down and explain each of the equations one by one.

Equation 1: Continuity Equation

$$\frac{\tilde{\partial}\,\tilde{u}}{\tilde{\partial}\,\hat{x}} + \frac{\tilde{\partial}\,\tilde{v}}{\tilde{\partial}\,\hat{y}} + \frac{\tilde{\partial}\,\tilde{w}}{\tilde{\partial}\,\hat{z}} = 0$$

This equation represents the continuity equation for an incompressible fluid. It states that the divergence of the velocity field $\tilde{u}, \tilde{v}, \tilde{w}$ is zero, implying that the fluid density remains constant within a flow. In simpler terms, it ensures that the mass of the fluid is conserved as it flows.

Equation 2: Navier-Stokes Equation (x-component)

$$v\frac{A}{C}\frac{\tilde{\partial}^2\tilde{u}}{\tilde{\partial}\tilde{z}^2} + v\frac{A}{2C^3}\left(\frac{\tilde{\partial}\tilde{u}}{\tilde{\partial}\tilde{z}}\right)^2\frac{\tilde{\partial}^2\tilde{u}}{\tilde{\partial}\tilde{y}^2} + \frac{\sigma\hat{B}_0^2\tilde{u}}{\hat{\rho}\,(\alpha_h^2+\alpha_i^2)}(\alpha_h\hat{v} - \alpha_i\hat{u}) = \tilde{u}\frac{\tilde{\partial}\tilde{u}}{\tilde{\partial}\tilde{x}} + \tilde{v}\frac{\tilde{\partial}\tilde{u}}{\tilde{\partial}\tilde{y}} + \tilde{w}\frac{\tilde{\partial}\tilde{u}}{\tilde{\partial}\tilde{z}}$$

This is the x-component of the Navier-Stokes equation with additional terms that might represent magnetic field effects, nonlinear terms, and other complexities.

a. ν represents the kinematic viscosity.

b. The term $\frac{\tilde{\partial}^2\tilde{u}}{\tilde{\partial}\tilde{z}^2}$ represents the diffusion of momentum in the z-direction.

c. The nonlinear term $(\frac{\tilde{\partial}\tilde{u}}{\tilde{\partial}\tilde{z}})^2 \frac{\tilde{\partial}^2\tilde{u}}{\tilde{\partial}\tilde{y}^2}$ represents interactions between different components of the flow.

d. The magnetic term $\frac{\sigma\hat{B}_0^2\tilde{u}}{\hat{\rho}\,(\alpha_h^2+\alpha_i^2)}(\alpha_h\hat{v} - \alpha_i\hat{u})$ represents the effects of a magnetic field on the flow.

e. The terms on the right side $\tilde{u}\frac{\tilde{\partial}\tilde{u}}{\tilde{\partial}\tilde{x}} + \tilde{v}\frac{\tilde{\partial}\tilde{u}}{\tilde{\partial}\tilde{y}} + \tilde{w}\frac{\tilde{\partial}\tilde{u}}{\tilde{\partial}\tilde{z}}$ represent the convection of momentum.

Equation 3: Navier-Stokes Equation (y-component)

$$\tilde{u}\frac{\tilde{\partial}\tilde{v}}{\tilde{\partial}\hat{x}} + \hat{v}\frac{\tilde{\partial}\tilde{v}}{\tilde{\partial}\hat{y}} + \tilde{w}\frac{\tilde{\partial}\tilde{v}}{\tilde{\partial}\hat{z}} = v\frac{A}{C}\frac{\tilde{\partial}^2\tilde{v}}{\partial\,\bar{z}} + v\frac{A}{2C^2}(\frac{\tilde{\partial}\tilde{v}}{\tilde{\partial}\bar{z}})^2\frac{\tilde{\partial}^2\tilde{v}}{\tilde{\partial}\hat{y}^2} - \frac{\hat{\sigma}\hat{B}_0^2\tilde{v}}{\hat{\rho}\,(\alpha_h^2+\alpha_i^2)}(\alpha_h\hat{v} - \alpha_i\hat{u})$$

This is the y-component of the Navier-Stokes equation with similar terms as in the x-component, indicating the dynamics of the velocity component ˜vin the y-direction.

Equation 4: Energy Equation

$$\rho^* C_P\left[\tilde{u}\frac{\partial\tilde{T}}{\partial\tilde{x}} + \tilde{v}\frac{\partial\tilde{T}}{\partial\tilde{y}} + \tilde{w}\frac{\partial\tilde{T}}{\partial\tilde{z}}\right] = -\nabla.q^*$$

This equation represents the energy conservation in the fluid, where:

a. ρ* is the density.

b. Cp is the specific heat capacity at constant pressure.

c. $\tilde{T}$ is the temperature.

d. -q* is the heat flux.

The left-hand side represents the convective transport of energy, and the right-hand side represents the divergence of the heat flux.

Equation 5: Species Transport Equation

$$\tilde{u}\frac{\partial\tilde{C}}{\partial\tilde{x}} + \tilde{v}\frac{\partial\tilde{C}}{\partial\tilde{v}} + \tilde{w}\frac{\partial\tilde{C}}{\partial\tilde{z}} = -\nabla.J^*$$

This equation describes the transport of a species concentration $\tilde{C}$:

a. $\tilde{u}, \tilde{v}, \tilde{w}$ are velocity components. -J* is the diffusive flux of the species.

The left-hand side represents the convective transport of the species, and the right-hand side represents the diffusion.

Equation 6: Generalized Heat Flux Equation

$$q^* + \gamma_1^*\left[\frac{\tilde{\partial}q^*}{\tilde{\partial}t} + (\nabla.\ V)q^* - q^*.\nabla\,\mathrm{V} + \mathrm{V}.\nabla\mathrm{q}^*\right] = -K^{***}\nabla.\tilde{T}$$

This equation models the heat flux q*:

a. $\gamma_1^* is\ a\ relaxation\ time\ or\ related\ parameter$
b. K*** is a thermal conductivity term.
c. The bracketed term involves time derivative, divergence of velocity field, and convective terms affecting q*.

Equation 7: Generalized Mass Flux Equation

$$J^* + \gamma_2^* \left[\frac{\tilde{\partial} J^*}{\tilde{\partial} t} + (\nabla .\ V) J^* - J^* . \nabla \mathrm{V} + \mathrm{V} . \nabla \mathrm{J}^* \right] = -D^{***} \nabla . \tilde{C}$$

This equation models the mass flux J:

a. γ_2^* is a relaxation time or related parameter.
b. D*** is a diffusivity term.
c. The bracketed term involves time derivative, divergence of velocity field, and convective terms affecting J*.

Overall, these equations describe the dynamics of fluid flow, heat transfer, and species transport in a system, likely under the influence of magnetic fields and other complex interactions.

Conflict of Interest

The authors declare that they have no known competing financial interests or personal relationships that could have appeared to influence the work reported in this paper.

Funding

The research received no specific grant from any funding agency in the public, commercial, or not-for-profit sectors.

Data Fabrication/Falsification Statement

The author(s) declare that no data has been fabricated, falsified, or manipulated in this study.

Participant Consent

The authors confirm that Informed consent was obtained from all participants, and confidentiality was duly maintained.

References

[1] F. W. Twort, "An investigation on the nature of ultra-microscopic viruses,"Acta Kravsi, 1961.
[2] F. d'Herelle, "An invisible microbe that is antagonistic to the dysentery bacillus,"CR Acad Sci, vol. 165, pp. 373–375, 1917.
[3] T. R. Callaway, T. S. Edrington, A. Brabban, B. Kutter, L. Karriker, C. Stahl, E. Wagstrom, R. Anderson, T. L. Poole, K. Genovese,et al., "Evaluation of phage treatment as a strategy to reduce

salmonella populations in growing swine,"Foodborne pathogens and disease, vol. 8, no. 2, pp. 261–266, 2011.

[4] S. B. Cha, A. N. Yoo, W. J. Lee, M. K. Shin, M. H. Jung, S. W. Shin, Y. W. Cho, and H. S. Yoo, "Effect of bacteriophage in enterotoxigenic escherichia coli (etec) infected pigs," Journal of Veterinary Medical Science, vol. 74, no. 8, pp. 1037–1039, 2012. 23

[5] N. Stalin and P. Srinivasan, "Efficacy of potential phage cocktails against vibrio harveyi and closely related vibrio species isolated from shrimp aquaculture environment in the south east coast of india,"Veterinary Microbiology, vol. 207, pp. 83–96, 2017.

[6] J. Woolston, A. R. Parks, T. Abuladze, B. Anderson, M. Li, C. Carter, L. F. Hanna, S. Heyse, D. Charbonneau, and A. Sulakvelidze, "Bacteriophages lytic for salmonella rapidly reduce salmonella contamination on glass and stainless steel surfaces,"Bacteriophage, vol. 3, no. 3, p. e25697, 2013.

[7] K. I. Nkwe, C. N. Ateba, N. P. Sithebe, and C. C. Bezuidenhout, "Enumeration of somatic and f-rna phages as an indicator of fecal contamination in potable water from rural areas of the north west province,"Pathogens, vol. 4, no. 3, pp. 503–512, 2015.

[8] B. Wu, R. Wang, and A. G. Fane, "The roles of bacteriophages in membrane-based water and wastewater treatment processes: A review,"Water research, vol. 110, pp. 120–132, 2017.

[9] Z. Maimaiti, Z. Li, C. Xu, J. Chen, and W. Chai, "Global trends and hotspots of phage therapy for bacterial infection: A bibliometric visualized analysis from 2001 to 2021,"Frontiers in Microbiology, vol. 13, p. 1067803, 2023.

[10] E. E. Kyaw, H. Zheng, and J. Wang, "Stability and hopf bifurcation analysis for a phage therapy model with and without time delay,"Axioms, vol. 12, no. 8, p. 772, 2023.

[11] S. A. Gómez-Ochoa, M. Pitton, L. G. Valente, C. D. S. Vesga, J. Largo, A. C. QuirogaCenteno, J. A. H. Vargas, S. J. Trujillo-Cáceres, T. Muka, D. R. Cameron,et al., "Efficacy of phage therapy in preclinical models of bacterial infection: a systematic review and metaanalysis,"The Lancet Microbe, 2022.

[12] L. Blasco, I. López-Hernández, M. Rodríguez-Fernández, J. Pérez-Florido, C. S. CasimiroSoriguer, S. Djebara, M. Merabishvili, J.-P. Pirnay, J. Rodríguez-Baño, M. Tomás,et al., "Case report: Analysis of phage therapy failure in a patient with a pseudomonas aeruginosa prosthetic vascular graft infection,"Frontiers in Medicine, vol. 10, p. 1199657, 2023.

[13] L. Blasco, I. López-Hernández, M. Rodriguez-Fernandez, J. Perez-Florido, C. S. CasimiroSoriguer, S. Djebara, M. Merabishvili, J.-P. Pirnay, J. Rodriguez-Bano, M. Tomas,et al., 24 "Analysis of phage therapy failure in a patient with a pseudomonas aeruginosa prosthetic vascular graft infection,"medRxiv, pp. 2023–03, 2023.

[14] N. Cesta, M. Pini, T. Mulas, A. Materazzi, E. Ippolito, J. Wagemans, M. Kutateladze, C. Fontana, L. Sarmati, A. Tavanti,et al., "Application of phage therapy in a case of a chronic hip-prosthetic joint infection due to pseudomonas aeruginosa: an italian real-life experience and in vitro analysis," inOpen Forum Infectious Diseases, vol. 10, p. ofad051, Oxford University Press US, 2023.

[15] A. S. Perelson and P. W. Nelson, "Mathematical analysis of hiv-1 dynamics in vivo,"SIAM review, vol. 41, no. 1, pp. 3–44, 1999.

[16] M. Nowak and R. M. May,Virus dynamics: mathematical principles of immunology and virology: mathematical principles of immunology and virology. Oxford University Press, UK, 2000.

[17] E. E. Kyaw, H. Zheng, and J. Wang, "Stability and hopf bifurcation analysis for a phage therapy model with and without time delay,"Axioms, vol. 12, no. 8, p. 772, 2023.

[18] D. Ebert, M. Lipsitch, and K. L. Mangin, "The effect of parasites on host population density and extinction: experimental epidemiology with daphnia and six microparasites,"The American Naturalist, vol. 156, no. 5, pp. 459–477, 2000.

[19] X. Li, R. Huang, and M. He, "Dynamics model analysis of bacteriophage infection of bacteria,"Advances in Difference Equations, vol. 2021, pp. 1–11, 2021.

[20] P. Van den Driessche and J. Watmough, “Reproduction numbers and sub-threshold endemic equilibria for compartmental models of disease transmission,”Mathematical biosciences, vol. 180, no. 1-2, pp. 29–48, 2002.

[21] G. Fabiani, E. Galaris, L. Russo, and C. Siettos, “Parsimonious physics-informed random projection neural networks for initial value problems of odes and index-1 daes,”Chaos: An Interdisciplinary Journal of Nonlinear Science, vol. 33, no. 4, 2023.